Available online at www.sciencedirect.com
ScienceDirect
Journal of Nuclear Materials 358 (2006) 106–110
journal of nuclear materials
www.elsevier.com/locate/jnucmat

Porosity influence on the mechanical properties of polycrystalline zirconium nitride ceramics

Jun Adachi *, Ken Kurosaki, Masayoshi Uno, Shinsuke Yamanaka

Division of Sustainable Energy and Environmental Engineering, Graduate School of Engineering, Osaka University, Yamadaoka 2-1, Suita, Osaka 565-0871, Japan

Received 15 March 2006; accepted 9 July 2006

Abstract

Polycrystalline zirconium nitride (ZrN) pellets, which have three kinds of porosity but have the same grain size, were prepared by the spark plasma sintering (SPS). The room temperature mechanical properties of the samples were evaluated by ultrasonic pulse echo measurements, Vickers hardness tests and nanoindentation tests. The general equations for the porosity influence on Young's modulus and hardness were proposed.

PACS: 62.20.Dc; 62.20.−X

1. Introduction

Zirconium nitride (ZrN) is being studied as an inert matrix of actinide targets of accelerator driven system (ADS) [1], because of its superior thermal, neutronic and chemical properties for a nuclear fuel cycle. For example, it has high melting temperature, high thermal conductivity, low creep rate and high chemical compatibility with SUS 316 stainless steel and liquid Na [2–4]. In addition, ZrN is a good candidate for ceramics coating films because it exhibits the excellent mechanical characteristics [5,6].

However, the thermophysical properties of ZrN have been scarcely evaluated because it is very difficult to prepare the high-density bulk samples. Therefore, most of the researches on the physical properties of ZrN have been performed on thin films [5–7]. In the present study, we prepared the polycrystalline sintered pellets of ZrN with various densities (in other words, various porosities) and measured the mechanical properties such as Young's modulus, Vickers hardness and nanoindentation hardness. From the experimental results, the influences of porosity on mechanical properties of ZrN were evaluated. Load dependence was also evaluated for hardness.

2. Experimental procedure

2.1. Sample preparation and characterization

The crystal structure and lattice parameter of ZrN powder (99.9%, Soekawa Chemical Co. Ltd.)

* Corresponding author. Tel.: +81 6 6879 7905; fax: +81 6 6879 7889.
E-mail address: j-adachi@stu.nucl.eng.osaka-u.ac.jp (J. Adachi).

0022-3115/$ - see front matter
doi:10.1016/j.jnucmat.2006.07.002

were evaluated by powder X-ray diffraction (XRD) method using Cu-Kα radiation at room temperature. The powder was placed into a 20 mm diameter graphite die and sintered by the spark plasma sintering (SPS, SUMITOMO COAL MINING Dr Sinter SPS-1020 apparatus) at 1773, 1873 and 2073 K each at the heating rate of 100 K/min in a nitrogen atmosphere. The bulk density of the sintered samples was determined by a geometric measurement. Mirror polish was performed on the bulk samples using SiC polishing papers and alumina colloidal powders whose grain sizes were 1.0, 0.3 and 0.05 μm. For the bulk samples, the shape and size of the grains and pores were evaluated with a scanning electron microscope (SEM, HITACHI S-2600H) and an optical microscope (OLYMPUS BX51M). The surface roughness was determined with an atomic force microscope (AFM, JEOL JSPM-4200).

2.2. Mechanical property measurements

The longitudinal and shear sound velocities were measured by the ultrasonic pulse–echo method (NIHON MATECH Echometer 1062) at room temperature in air. Various elastic moduli such as Young's modulus and shear modulus can be calculated from the measured sound velocities.

Vickers hardness was measured with a micro-Vickers hardness tester (MATSUZAWA SEIKI MHT-1) at room temperature in air. Applied load and loading time were chosen to be 0.98, 2.94 and 9.8 N, and 15 s, respectively. This measurement method follows JIS R1610.

The nanoindentation tests were performed at room temperature in air using an AFM with a nanoindenter (Hysitron Inc. TriboScope) for the sample prepared by SPS at 2073 K. The nanoindentation loads were chosen to be 2000, 4000 and 6000 μN. In the nanoindentation tests, the loading and unloading time, were chosen to be 5 s, each. According to the method of Oliver and Pharr [8], the load–displacement data obtained by nanoindentation tests enable us to calculate nanoindentation hardness (H_n) and reduced modulus (E_r). Young's modulus can be calculated from the following equation:

$$\frac{1}{E_r} = \frac{1-\nu_i^2}{E_i} + \frac{1-\nu_S^2}{E_S}, \tag{1}$$

where E and ν are Young's modulus and Poisson's ratio, and the subscripts of s and i represent a sample and an indenter, respectively. Young's modulus (E_i) and Poisson's ratio (ν_i) of the diamond tip are 1140 GPa and 0.07, respectively.

3. Results and discussion

3.1. Sample characteristics

From the powder XRD patterns of the samples at room temperature of the samples, it was confirmed that a single phase of ZrN with a NaCl type cubic structure was obtained in the present study. Lattice parameter evaluated from the XRD pattern is $a = 0.4586$ nm, which is consistent with the literature value (=0.4585 nm) [9]. The relative densities of the bulk type samples are 82.2, 91.3 and 93.4% T.D. for the SPS temperatures of 1773, 1873 and 2073 K, respectively. From the SEM and optical microscope observation results, the following two facts were confirmed. First, the grain size of the bulk sample is almost the same as that of one another in spite of the different sintering temperature because the sintering time is very short in the SPS process. In other words, the grain size of the powder sample before SPS corresponds to that of the bulk sample after the SPS. Therefore, the grain growth did not occur during the SPS process and so the grain sizes are comparable among the three bulk samples. Actually, the grain size was observed to be 10–20 μm. Second, the shape of pores is nearly spherical and the size of the pores is ≈1–2 μm. In addition, most of the pores concentrate along the grain boundaries. The sample characteristics are summarized in Table 1.

Fig. 1(a) and (b) shows the indentation images of the micro-Vickers indentation and nanoindentation, respectively. From these figures, the nanoindentation size is of a sub-micro scale, which is remarkably smaller than the grain size. In this case, the nanoindentation is scarcely affected by the porosity [10,11] because the nanoindentation is just performed in the grain. For instance, the diamond tip does not touch the grain boundary or the pores. Therefore, it is assumed that the results obtained from the nanoindentation tests represent mechanical properties of the porosity-free materials. From AFM analysis, the arithmetic average of surface roughness of the bulk samples was detected to be below 5 nm, which is extremely low compared to the contact depth of the nanoindentation tests.

Table 1
Sample characteristics and mechanical properties of ZrN

Sintering temperature (K)	1773	1873	2073
Relative density (% T.D.)	82.2	91.3	93.4
Crystal structure	NaCl type		
Lattice parameter at R.T. (nm)	0.4586		
Grain size (μm)	10–20	10–20	10–20
Pore size (μm)	1–2	1–2	1–2
Arithmetic average roughness (nm)	3.7	4.9	4.6
Longitudinal sound velocity (m/s)	5561	7126	7196
Shear sound velocity (m/s)	3335	4066	4135
Young's modulus[a] (GPa)	156	275	288
Shear modulus (GPa)	64	109	115
Bulk modulus (GPa)	92.7	190	195
Poisson ratio	0.219	0.259	0.253

[a] Young's modulus was obtained by the ultrasonic pulse echo measurement.

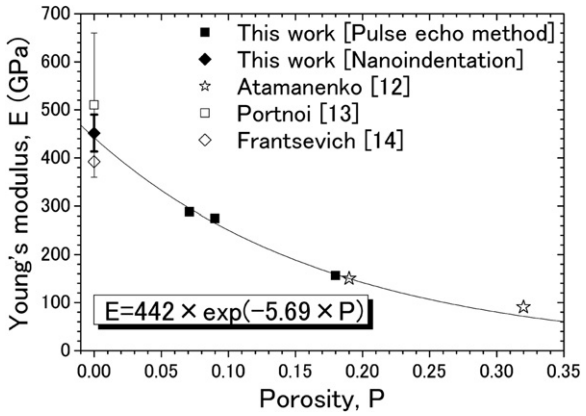

Fig. 2. Porosity dependence of Young's modulus of ZrN, together with the literature data [12–14].

3.2. Mechanical properties

3.2.1. Young's modulus

The values of sound velocities and elastic moduli obtained from the ultrasonic pulse echo measurements are summarized in Table 1. Fig. 2 shows the porosity dependence of Young's modulus obtained from the ultrasonic pulse echo measurements and the nanoindentation tests, together with the literature data [12–14]. The following equation suggested by Wachtman Jr. [15] describes the porosity dependence of Young's modulus:

$$E(P) = E_0 \exp(-aP), \tag{2}$$

where E_0 is Young's modulus of a porosity-free material, a is a constant, and P is the porosity. In Fig. 2, the results of Young's modulus obtained from the ultrasonic pulse echo measurement were represented by Eq. (2) and we obtained the following equation:

$$E(P)(\mathrm{GPa}) = 442 \times \exp(-5.69 \times P) \quad (0 < P < 0.2). \tag{3}$$

The value of E_0 (=442 GPa) is very close to the result obtained from the nanoindentation tests (=452 GPa). This result proves that the Young's modulus obtained from the nanoindentation tests represents the value of the porosity-free material.

3.2.2. Hardness

Fig. 3 shows the porosity dependence of the Vickers hardness at the loads of 9.8, 2.94 and 0.98 N, together with the literature data [16]. The following equation suggested by Luo [17] describes the porosity dependence of Vickers hardness:

$$H_V(F,P) = H_{V,0}(F) \times \exp(-b(F) \times P), \tag{4}$$

where $H_{V,0}$ is Vickers hardness of a porosity-free material, b is a constant that depends on the applied load, and P is the porosity. In Fig. 3, only the results of Vickers hardness obtained in the present study

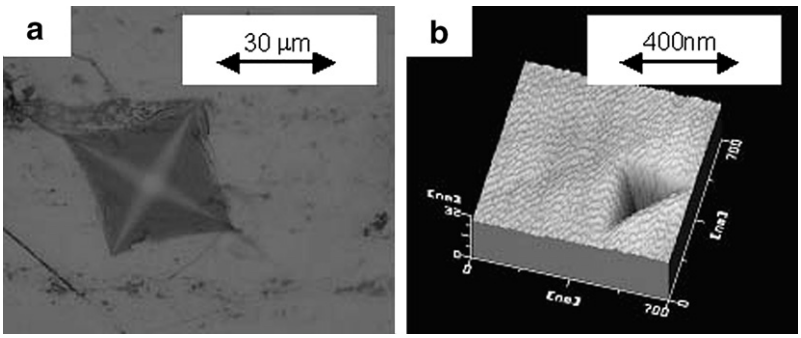

Fig. 1. Indentation image (a) micro-Vickers indentation (metallographic picture) and (b) nanoindentation (AFM image).

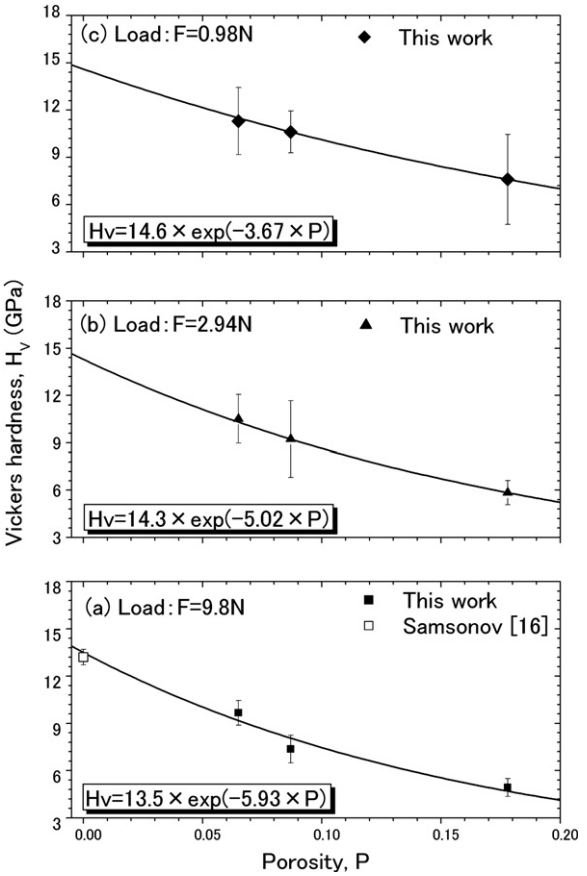

Fig. 3. Porosity dependence of hardness of ZrN, together with the literature data [16].

were represented by Eq. (4) and the following equations were obtained:

$$H_V(9.8\,N,P)(GPa) = 13.5 \times \exp(-5.93 \times P) \quad (0 < P < 0.2), \tag{5}$$

$$H_V(2.94\,N,P)(GPa) = 14.3 \times \exp(-5.02 \times P) \quad (0 < P < 0.2), \tag{6}$$

$$H_V(0.98\,N,P)(GPa) = 14.6 \times \exp(-3.67 \times P) \quad (0 < P < 0.2). \tag{7}$$

In Eq. (5), the estimated value ($=H_{V,0}(9.8\,N) =$ 13.5 GPa) of the Vickers hardness for the porosity-free material under the load of 9.8 N is nearly consistent with the experimental value (=13.2 GPa) reported in the literature [16]. Therefore, it is considered that the porosity dependence of Vickers hardness under the load of 9.8 N could be described by Eq. (5), accurately. Based on this, it is thought that $H_{V,0}(2.94\,N)$ and $H_{V,0}(0.98\,N)$ in Eqs. (6) and (7) should be consistent with the values of Vickers hardness for the porosity-free material under the loads of 2.94 N and 0.98 N, respectively. In addition, the b value decreases with decreasing load. This indicates that the porosity influence on the hardness decreases with decreasing load.

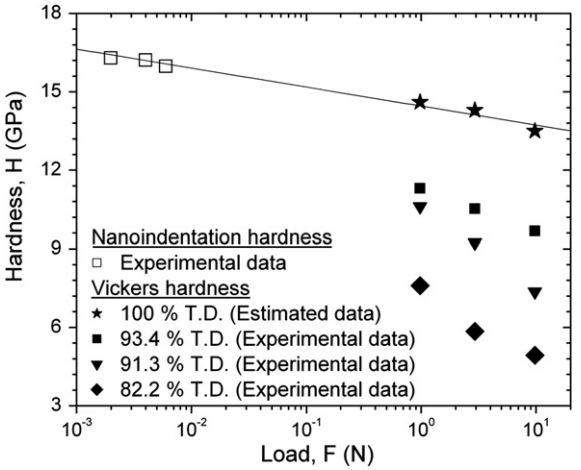

Fig. 4. Load dependence of hardness of ZrN.

Fig. 4 shows the load dependence of Vickers hardness and nanoindentation hardness of ZrN. In this figure, the estimated values of Vickers hardness using Eqs. (5)–(7) are shown as solid stars. From Fig. 4, it is found that the hardness decreases with increasing load. In the case of the nanoindentation hardness (H_n), nanoindentation hardness decreases with increasing load, according to the indentation size effect [18]. In the case of Vickers hardness (H_V), the number of cracks occurring from Vickers indentation increases with increasing load. This leads to the decrease of Vickers hardness arising from an increasing load.

4. Conclusion

The polycrystalline ZrN samples with various densities were prepared by SPS and their mechanical properties were measured.

From the ultrasonic pulse echo measurements, the following equation, which represents the porosity dependence of Young's modulus of ZrN, was obtained:

$$E(P)(GPa) = 442 \times \exp(-5.69 \times P) \quad (0 < P < 0.2),$$

in which 442 means Young's modulus of the porosity-free material. 442 GPa is consistent with the value obtained from the nanoindentation test, i.e., 451 GPa. It is found that the nanoindentation is a very effective method to evaluate the mechanical

properties not only of thin films and/or single crystalline but also of polycrystalline ceramics.

From the results of Vickers hardness tests, the following equation, which represents the porosity dependence of Vickers hardness of ZrN, was obtained:

$$H_V(9.8\,\mathrm{N},P) = 13.5 \times \exp(-5.93 \times P) \quad (0 < P < 0.2),$$

in which 13.5 means hardness of the porosity-free material. The nanoindentation hardness and Vickers hardness decrease with increasing load due to the indentation size effect and increasing the crack density, respectively.

In the present study, Young's modulus and hardness of ZrN were able to be evaluated systematically, and the equations for the porosity effect on Young's modulus and hardness were obtained. These equations allow us to calculate Young's modulus and hardness under various sample characteristics and measurement conditions.

References

[1] H. Matzke, Science of Advanced LMFBR Fuels, Elsevier Science Publishers Co., New York, 1986.
[2] A. A. Bauer, P. Cybulskis, J. L. Green, Mixed-nitride fuel performance in EBR-II, in Adv. LMFBR Fuels Top. Meet, in: Proc., Columbus, OH, Edited by Am. Nucl. Soc. (1977) 299.
[3] D. Brucklacher, Fak. Maschinenbau, Fed. Rep. Ger. Avail. INIS. Report, INIS-mf-5402 (1978) 101.
[4] A.K. Sengupta, C. Ganguly, Trans. Indian Inst. Met. 43 (1) (1990) 31.
[5] A. Mitsuo, T. Mori, Y. Setsuhara, S. Miyake, T. Aizawa, Nucl. Instrum. Meth. Phys. Res. Sect. B 206 (2003) 366.
[6] E. Atar, C. Sarioglu, U. Demirler, E.S. Kayali, H. Cimenoglu, Scripta Mater. 48 (2003) 1331.
[7] M. Chhowalla, H.E. Unalan, Nature Mater. 4 (4) (2005) 317.
[8] W.C. Oliver, G.M. Pharr, J. Mater. Res. 7 (6) (1992) 1564.
[9] JCPDS card, 2-956 (ZrN).
[10] B. Jang, H. Matsubara, Mater. Lett. 59 (27) (2005) 3462.
[11] R.G. Wellman, A. Dyer, J.R. Nicholls, Surf. Coat. Tech. 176 (2) (2004) 253.
[12] B.A. Atamanenko, Phys. Chem. Mech. Surf. 9 (1995) 281.
[13] K.I. Portnoi, A.A. Mulaseev, V.N. Gribkov, Yu.V. Levinskii, Soviet Powder Metall. Met. Ceram. 8 (5) (1968) 406.
[14] I.N. Frantsevich, E.A. Zhurakovskii, A.B. Lyashchenko, Neorgan. Mat. 3 (1) (1967) 8.
[15] J.B. Wachtman Jr., Bureau of Standards Spec. Pub. 303 (1968) 139.
[16] G.V. Samsonov, I.M. Vinitskii, Handbook of refractory compounds, IFI/Plenum, New York, 1980.
[17] J. Luo, R. Stevens, Ceram. Int. 25 (1999) 281.
[18] A.C. Fisher-Cripps, Nanoindentation, Springer, New York, 2002, p. 74.